Effect of hydrodynamic cavitation on zooplankton: a tool for disinfection

Subhash Shivram Sawant,[a] Arga Chandrashekar Anil,[a*] Venkat Krishnamurthy,[a] Chetan Gaonkar,[a] Janhavi Kolwalkar,[a] Lidita Khandeparker,[a] Dattesh Desai,[a] Amit Vinod Mahulkar,[b] Vivek Vinayak Ranade,[c] Aniruddha Balchandra Pandit,[b]

[a] National Institute of Oceanography, Dona Paula, Goa – 403 004, India

[b] Institute of Chemical Technology, University of Mumbai, Mumbai - 400 019, India

[c] National Chemical Laboratory, Pune 411 008, India

Abstract

Application of hydrodynamic cavitation for disinfection of water is gaining momentum, as it provides environmentally and economically sound options. In this effort, the effect of cavitating conditions created by differential pump valve opening and that created by flowing through a cavitating element (orifice plates) on the microbes (zooplankton in seawater) is described. The experimental results are compared with modeling of cavitating conditions that includes cavity dynamics, turbulence generated by individual oscillating cavity, cell wall strength and geometrical & operating parameters of cavitation device. Theoretical model for quantifying the cavitationally generated turbulent shear and extent of microbial disinfection has been developed. Experimental results indicated that cavitation and/or turbulent fluid shear dominantly originating from cavitation are effective tools for seawater disinfection as more than 80% of the Zooplankton present in the seawater were killed. It was also observed that shock waves generated due to cavitation is not the sole cause for zooplankton disruption. A correct physical mechanism accounting fluid turbulence and shear, generated from stable oscillation of cavity, significantly contribute towards the disruption. Further refinement of the model presented will serve as a basis for higher degree of disinfection and provide a practical tool for sea water disinfection.

Keywords: Cell Disruption; Hydrodynamic Cavitation; Zooplankton; Modelling; Heat Transfer; Wastewater Treatment

1. Introduction

Cavitation is a phenomenon of formation, growth and collapse of micro bubbles within a liquid. In hydrodynamic cavitation, the pressure variation in the flowing liquid causes cavitation. Vaporous cavity can form anywhere in a flowing liquid where the local pressure is reduced to that of the liquid vapor pressure at the temperature of the flowing liquid [1]. The condition at which these fine bubbles are produced is termed as cavitation inception. An increase in the velocity will result in a further drop in pressure and an increase in number density of cavities. Pressure recovery takes place further downstream where these cavities collapse violently thereby generating a high magnitude pressure pulse. If the gas content inside the cavity is small enough, the pressure impulse could be very high, of the order of several hundreds of bars [2], which is sufficiently high to rupture the biological constituents of water including the microbial cells causing its destruction [3]. Asymmetric collapse of cavities also results in high-speed liquid jets. Shear rates around such jets is adequate to kill, even, microorganisms. This technology can serve in remediation and disinfection of the wastewater generated by different anthropogenic activities. Apart from making contaminated water into potable one for drinking purpose, it can find utility in treating ship's ballast water. Shipping is the backbone of global economy and facilitates transportation of 90% of the commodities. It is estimated that 2–3 billion tonnes of ballast water is carried around the world each year. Translocation of organisms through ships (bio-invasion) is considered to be one of the important issues that threaten the naturally evolved biodiversity, the consequences of which are being realized increasingly in the recent years [4]. While many treatment technologies such as self-cleaning screen filtration systems, ozonation, de-oxygenation,

electro-ionization, gas super saturation, chemical treatments etc. are being tried, they cannot limit the environmentally hazardous effects that could result from such practices. Hydrodynamic Cavitation has been successfully applied for water disinfection, enzyme recovery and wastewater treatment [3, 5, 6]. Hydrodynamic cavitation can be easily scaled up for operation on very large scale especially as required for ballast water treatment. As per the current knowledge of authors no previous work has been reported which explores the utility of hydrodynamic cavitation in eradication of marine zooplankton particularly directed towards Ballast water treatment.

2. Materials and methods

2.1. Experimental set-up

A schematic of the experimental setup is shown in Fig. 1. Setup consisted of feed tank (A), Centrifugal Pump 7.5 hp (B), valve (C), Pressure gauge (D), cavitation element orifice plate (E), collection tank (F). Pipe diameter was 26 mm. It is a well known fact that cavitation can also occur in partially closed valve or a centrifugal pump under certain operating conditions. Hence, it is likely that zooplanktons might also get killed in pump or even valve. Thus, in order to quantify the cavitation effects occurring only inside the orifice plates and to relate it to the extent of zooplanktons disruption, the experiments were carried out with and without cavitation element (orifice plate). First experiment (control run) was performed by pumping the sea water from feed tank (A) to collection tank (E) through a fully open valve and without orifice plate being placed in line (Case VI in Table 1). Another two set of experimental runs were carried out for two different open area of valve (20% & 40% open area) without orifice plate being placed in line

(Case IV & V in table 1). Results from this experiment quantified the effectiveness of valve in generating cavitation and quantified zooplankton that would be killed inside the partially closed valve. Subsequently three more sets of experiments were carried out for three different open areas of orifice plates (25%, 50% & 75% open area), (Case I, II & III in table 1). The configuration of the constrictions (orifice plates & valves) is shown in Fig. 2. In all the experiments sea water was passed just once through the cavitation device. (Table 1 here)

Seawater was first collected and stored in (storage tank A). Subsequently, the seawater was inoculated with concentrated zooplankton sample collected from the Dona Paula Bay (Goa, India). This Challenged water in the storage tank (A) with the concentrated zooplankton inoculum was evaluated for the abundance of live organisms. (Fig 1. & 2. here)

2.2. Evaluation of zooplankton survival rate

Zooplankton of size greater than 50μ was assessed in the intake (pre-cavitation condition) and discharge (post-cavitation condition) waters. For this purpose, a known volume of intake water and discharge water was filtered separately through a sieve made up of bolting silk with 50μ mesh. The Zooplankton retained on the sieve was transferred immediately into a known volume of filtered seawater. The observation from the storage tank is considered as the initial concentration of organisms. Fifty liters (50 l) of water was sampled thrice in each of the experimental conditions and the numbers of live organisms were quantified from six sub samples from each of the replicate (n= 3x6). Only live organisms (with mobility) were enumerated using a binocular microscope. This number is expressed as individuals per cubic meter. The numbers of live individuals were

classified into different taxonomic units as indicated in the relevant figures. The live
zooplankton count in discharge water is compared with intake water and the percentage
killing of number of planktons is calculated using the following formula:

$$\text{Killing (\%)} = \frac{(I - D)}{I} * 100 \tag{1}$$

Where, I = Cell count in intake water (pre-cavitation)

D = Cell count in discharge water (post-cavitation)

3. Cavitation number and its relevance to the energy delivered to the cavitating system

Applying Bernoulli's theorem at point 2 (vena contracta) & point 3 (downstream
the orifice) as shown in figure 3.

$$\frac{P_2}{\rho g} + \frac{V_2^2}{2g} + Z_2 = \frac{P_3}{\rho g} + \frac{V_3^2}{2g} + Z_3 \tag{2}$$

Since the locations 2 & 3 are geometrically close to each other we can neglect the
difference between the potential heads ($Z_2 \sim Z_3$). For an orifice with 5% open area & pipe
velocity (point 3) of 0.5 m/s, the velocity at point 2 (orifice) is of order of 10 m/s thus the
velocity head at point 3 is negligible as compared to that at point 2. On canceling the
potential head terms and velocity head terms at point 3 and rearranging the equation we
get

$$\frac{P_3 - P_2}{\frac{1}{2}\rho V_2^2} = 1 \tag{3}$$

It means that all the pressure head and velocity head at point 2 is recovered in the form of
pressure head at point 3. But this is true only in case of single phase system i.e. in

4

absence of cavitation or flashing. When cavitation takes place in the system, some liquid energy is lost in generation of secondary vapour phase. Hence, the pressure head obtained at point 3 is lesser than the sum of velocity head and pressure head at point 2. The difference in heads of liquid energy at these two points is representative of the extent of cavitation taking place. Thus, in the case of cavitation taking place, left hand side in equation 3 is less than one. When cavitation occurs in the system the pressure at point 2 is equal to vapour pressure of the liquid because the liquid has tendency to flash into vapour when subjected to bulk pressure lesser than its vapour pressure. Thus the pressure at point 2 is taken as vapour pressure of the liquid, & cavitation number is defined as

$$C_{vn} = \frac{P_3 - P_v}{\frac{1}{2} \rho V_2^2}$$
(4)

When cavitation number is greater than 1, it means that the liquid is resistant to the cavitation. When cavitation number is less than 1, it means that fluid energy (velocity head and pressure head at constriction) is being taken for the creation of vapour phase and hence cavitation. Thus, lower the cavitation number, higher is the quantity of energy taken for the cavitation process and more is its intensity. Impurities present in the liquid aid the process of formation of vapour phase, thus every time it is not essential to lower the pressure over the liquid for cavitation to occur. Hence cavitation also occurs when cavitation number is greater than one (Cavitation number > 1) [7].

(Fig. 3 here)

4. Mechanism of cavitationally induced cell disruption

Several mechanisms of cell disruption occurring due to cavitation are reported. Engler & Robinson [8], based on their experiments on high pressure homogenizer, stated that impingement of a high velocity jet of suspended cells on a stationary surface is

necessary for effective disruption of cell walls. Keshavarz et. al. [9] proposed similar mechanism of impingement for cell disruption in high pressure homogenizer. For cavitation based cell disruption method, Save et. al. (1994) [3] has proposed that shock wave i.e. the pressure impulse produced from the collapsing cavities is the main cause for cell disruption. Doulah [10] explained the mechanism of cavitationally induced cell disruption based on Kolmogoroff's [11] theory of isotropic turbulence and on analysis of fluid eddies created due to the collapse of cavity. The fluid eddies smaller than the dimension of cell will impart motions of various intensities to it, and when kinetic energy content of a cell exceeds the wall strength, the cell disintegrates.

Although, most of the above stated mechanisms of cell disruption are based on cavitation but their exact mechanisms of action is very different. Because of inadequacy of current experimental techniques to closely monitor/ observe the cavitational phenomena in real system, which occurs in extremely small time and length scales, it is difficult to conclude as on which of the above cell disruption mechanism is correct. It is also possible that the cell disruption would take place by combination of several actions simultaneously like high velocity liquid jet, shock wave etc.

Thus, in the absence of any concrete information about the actual mechanism, we develop a mathematical correlation based on the net energy delivered by a cavity to the surrounding liquid and not on specific energy associated with liquid jet or shock wave. Before we develop the model let us consider cavity dynamics behavior under various circumstances.

Consider a cavity to collapse near a solid surface, in such a case the cavity tends to become asymmetric and takes the form of a rapidly accelerating jet of fluid, entering

the bubble from the side furthest from the wall, which results, into asymmetric collapse of cavity, thus creating a high velocity liquid jet and fluid eddies with high energy content [12, 13]. On the other hand, collapse of a cavity in bulk liquid away from solid boundaries results into symmetrical collapse. Symmetrical collapse produces extremely high pressure and temperature, which results into formation of shock waves. Presence of microbial cells, of size comparable to the size of cavity, near a cavity can also lead to asymmetric collapse.

Both, the symmetric and asymmetric collapse, deliver energy in different forms, i.e. either shock wave or liquid jet, but both the cavities deliver same net energy because it had received same quantity of energy from incident pressure fluctuations. Since all the energy, either delivered in the form of shock wave or liquid microjet, is in the end dissipated in liquid in the form of viscous dissipation and ultimately as thermal energy, we base our cell disruption model on viscous stress generated by the cavity on microbial cells. Action of viscous stress on microbial cell is already analyzed by Doulah [10] with acoustic cavitation for cell disruption. In the present case, the cell disruption model is based on the rate of turbulent energy delivered by the cavity to the surrounding liquid, thus we limit our analysis to spherical bubble dynamics. Spherical bubble dynamics also give an added advantage that the cavity dynamics models for spherical cavity are much simpler (1-dimensioanl ordinary differential equation) as compared to those for non-spherical cavity dynamics (3-dimensioanl partial differential equations). In the next section we discuss the solution to cavity dynamics models and a numerical method to estimate the turbulent shear stress produced by a single cavity, which is obtained from bubble dynamics equation. Thereafter, a correlation is proposed which predicts the extent

of killing of zooplankton based on the turbulence shear stress generated by individual cavity, geometry of cavitation element (orifice plate/ valve) and operating conditions therein.

5. Numerical model

5.1 Cavity dynamics model

The dynamics of cavity is modeled using Rayleigh-Plesset equation, developed by Rayleigh [14] and later modified by Plesset [15] and the Tomita-Shima equation [16]. Heat transfer between the liquid and cavity is also considered and it also incorporates the latent heats of phase change. Mass transfer of condensable vapour to the bulk liquid is also included.

A cavity moving in the flowing liquid experiences a turbulent fluctuating pressure which causes the cavity to undergo volumetric oscillations. The Rayleigh-Plesset equation (Equ. 5) gives the dynamics of a spherical bubble, placed in an infinite liquid, as a function of changing internal bubble pressure, external liquid pressure, bubble radius, bubble wall velocity and liquid properties like surface tension, density and viscosity.

$$R(\frac{d^2R}{dt^2}) + \frac{3}{2}(\frac{dR}{dt})^2 = \frac{1}{\rho_l}\left[P_B - \frac{4\mu}{R}(\frac{dR}{dt}) - \frac{2\sigma}{R} - P_\infty \right]$$

(5)

Liquid phase Compressibility considerations [16] give the bubble dynamics equation represented in equation (6) and is considered as the second order approximation of the liquid phase compressibility. The liquid phase compressibility becomes significant during the bubble collapse, when bubble wall velocity reaches the velocity of sound in the liquid medium. In the present model, Rayleigh-Plesset equation (Eqn. 5) is used when bubble wall velocity is less than the velocity of sound and Tomita-Shima equation (Eqn.

6) is used when bubble wall velocity exceeds the velocity of sound to understand & model the cavity wall motion.

$$R\ddot{R}(1 - \frac{2\dot{R}}{C} + \frac{23\dot{R}^2}{10C^2}) + \frac{3}{2}\dot{R}^2(1 - \frac{4\dot{R}}{3C} + \frac{7\dot{R}^2}{5C^2}) +$$
$$\frac{1}{\rho_l}\left[\begin{array}{c} p_{\infty(t)} - F_{2(r=R)} + \frac{R}{C}(\dot{p}_{\infty(t)} - \dot{F}_{1(r=R)}) + \\ \frac{1}{C^2}\left\langle \begin{array}{c} -2R\dot{R}\left(\dot{p}_{\infty(t)} - \dot{F}_{1(r=R)}\right) + \frac{1}{2}(P_{\infty(t)} - \\ F_{1(r=R)})\left(\dot{R}^2 + \frac{3}{\rho_l}\left(P_{\infty(t)} - F_{1(r=R)}\right)\right) \end{array} \right\rangle \end{array}\right] = 0 \quad (6)$$

Where F_1 and F_2 as a function of R are given as follows:

$$F_{1(r=R)} = p_B - \frac{2\sigma}{R} - \frac{4\mu}{R}\dot{R} \quad (7)$$

$$F_{2(r=R)} = p_{1(r=R)} - \frac{4\mu}{3\rho C^2}(\dot{p}_{\infty(t)} - \dot{p}_{1(r=R)}) \quad (8)$$

5.2 Energy balance

As shown in Fig. 4, two thermal regions are modeled. First one is the central hot core where the temperature (T_B) during the bubble collapse rises adiabatically, second one is the vapor side cold boundary layer near the cavity-liquid interface. Temperature of bulk liquid (T_∞) is assumed to be constant and is obtained by taking energy balance over the bubble.

(Fig. 4 here)

5.3 Effect of fluid turbulence

The turbulence affects the bubble dynamics in a following ways.

a) The turbulent fluctuating pressure

9

The turbulent fluctuating pressures due to turbulent fluctuating velocities in the flowing liquid near the bubble affect the bubble dynamics. The turbulence pressure recovery downstream of an orifice is obtained based on the turbulence model proposed by Moholkar & Pandit (1997) [2]. The turbulence model calculates the amplitude of pressure fluctuation and turbulence frequency based on the power dissipation per unit mass of liquid downstream of the orifice.

b) The turbulent shear stress limits the size of bubble

The turbulent fluid shear stress limits the maximum size of the bubble that can remain stable. The Weber number criterion is used to relate the maximum size of the bubble to the turbulent fluctuating velocity [17]. Maximum size attained by bubble is restrained by critical Weber number (W_e) and the criterion is defined as (based on orifice flow).

$$W_e = \frac{2Rv'^2 \rho}{\sigma} = 4.7$$

(9)

It is assumed that bubble retains its size when restricted by the critical Weber number (W_e). When the bubble size becomes greater than critical size given by Weber number, than the bubble size reduces to critical size due to turbulent shear by the breakage of the bubble fragments.

5.4 Termination criterion

Cavity collapse criterion is based on material volume concept. Vander wall equation of state is given as

$$\left(P - \frac{an^2}{Vol^2}\right)(Vol - nb) = nRgT$$

(10)

Where, 'n' is number of moles and 'b' is the measure of excluded volume per mole of gas and can be regarded as the material volume per mole of gas. Therefore any gas cannot be compressed beyond its material volume which is given as 'bn'. Once the bubble volume reduces to the material volume of molecules present in it (bn), bubble (cavity) is said to be collapsed. After every iteration, the material volume of the then bubble content is calculated and compared to actual volume of the bubble. Simulation is terminated as soon as actual volume equals or becomes lesser than the material volume [18]. The cavity dynamics model equations are ordinary differential equations that are solved using Runge Kutta 4th order method.

5.5. Turbulent shear due volumetric oscillation of cavity

Cavity dynamics model predicts the instantaneous radius *R(t)*, bubble wall velocity *S(t)*, pressure inside the bubble $P_B(t)$, as the function of time varying liquid side pressure $P_\infty(t)$. When a cavity undergoes volumetric oscillations, the surrounding liquid is also set into radialy outwards (away from the centre of the cavity) and radially inwards (towards the centre of the cavity) motion. The instantaneous velocity of the liquid at distance R_{max} from the centre of cavity can be estimated as

$$v(t) = S(t)\frac{R^2(t)}{R_{max}^2} \tag{11}$$

Where R_{max} is the maximum radius reached by the cavity in its lifetime. The turbulence energy dissipation rate is calculated at distance R_{max} from the cavity because; this is the minimum possible distance between the oscillating cavity and a microbe.

The fluctuating velocity '*v*(t)' is correlated to the turbulence kinetic energy per unit mass '*k(t)*' of the liquid as

$$k(t) = \frac{1}{2}v^2(t) \tag{12}$$

The turbulence eddies generated from volumetric oscillation of cavity is typically of half the size of the cavity. Thus the eddy size 'l_{eddy}' can be estimated to be equal to time averaged radius of the cavity as

$$l_{eddy} = \overline{R} = \frac{\int_0^{t_{active}} R(t)dt}{\int_{00}^{t} t\,dt} \tag{13}$$

The instantaneous turbulence energy dissipation rates '$\varepsilon(t)$' can be estimated from the knowledge of instantaneous turbulence kinetic energy and typical turbulence eddy size as

$$\varepsilon(t) = \frac{k(t)^{3/2}}{l_{eddy}} \tag{14}$$

The time averaged value of turbulence energy dissipation rates ($\overline{\varepsilon}$) is calculated by taking the time average over the life time of cavity. The time average turbulent energy dissipation rate is related to stress that will be generated in surrounding liquid as [10]

$$\Delta P_{cavity} = (\rho\mu\overline{\varepsilon})^{1/2} \tag{15}$$

This stress generated by the cavity is related to the cell wall strength and will be used in the correlation to predict the extent of cell disruption.

6. Results & Discussion

From Table 1 we see that by simply pumping the sea water from tank A to tank E without placing any cavitation device (orifice plate) and keeping the valve completely open (control run, case VI), almost 28% of the zooplankton were killed. This means that

in spite of avoiding the cavitation (and shear generated by cavitation); the zooplankton are likely to be killed by turbulent shear generated by the flow of liquid inside the pump and not necessarily by cavitationally generated shear alone. Hence in this section, we first discuss the performance (ability to produce cavitation shear) of various designs of orifice plates and valves. Then we will discuss the effect of shear developed by turbulent liquid flow and shear generated by cavitation on the extent of disruption of zooplankton.

Shear generated by cavitation elements

Table 2 compares the cavitation number, time averaged turbulence energy dissipation rate of various cavitational devices under consideration. As said earlier in section 3 lesser value of cavitation number indicate that more energy is being dissipated in the liquid for generation of secondary phase (vapor phase), and hence greater is the intensity of cavitation. The same is also observed from the numerical simulations results. It is seen from table 2 that the least value of cavitation number is seen in case of valve with 20% open area (C_{vn}=1.93) where the average turbulence energy dissipation rate (ε=36994 m^2/s^3). While, the highest value of cavitation number is seen in the case of orifice with 75% open area (C_{vn}= 14.68) where the average turbulence energy dissipation rate (ε = 8717 m^2/s^3). This clearly indicates that the cavitation number predicts the relative intensity of cavitation taking place in various cavitation devices and can be used as preliminary tool to compare the relative performance of a cavitational system. (Table 2 here)

In case of 40% (open area) valve the cavitation number (C_{vn}=2.02) is lower than that of 25% orifice (C_{vn}=5.13), but still the average turbulence energy dissipation rate is

13

lower in case of valve with 40% open area. Such a variation can be explained based on the dynamics of the cavity in various cases (shown in Fig. 5). For a cavity to collapse intensely or to undergo rapid volumetric oscillation it should grow to a sufficiently large size and then collapse with greater bubble wall velocities. But in case of valve with 40% open area the high value of turbulent fluctuating velocities (2.06 m/s) does not permit the cavity to grow beyond 40μm as against the lower fluctuating velocity (1.27 m/s) generated in case of orifice with 25 % open area which permit relatively higher bubble sizes (100 μm). From figure 5 it is clearly evident that cavity in the case of orifice with 25% open area undergo volumetric oscillations of higher amplitude as compared to that in case of valve with 40% open area. Thus, the average turbulence energy dissipation rate is higher in case of orifice with 25% open area which is dominantly controlled by turbulent fluctuating velocities. It is evident from the above cavity dynamics analysis that cavities undergo violent volumetric oscillations which produces intense cavitational effects even in case of partially open valves. This is why substantial extent of killing of zooplankton (~50%) is seen to occur when sea water is passed through partially closed valves.

(Fig. 5 here)

Experimental results of zooplankton killing

As seen from table 2, almost 28% of the zooplankton was killed in the pump itself (case VI). This shows that the shear developed inside the pump is also capable of killing zooplankton. Still higher extent of killing of zooplankton (57% & 33%) was observed in partially closed valves (case IV & V). The highest extent of killing of zooplankton was observed for the cases of orifice plates (case I, II & III). It can be seen from table 2 that almost 82% of zooplankton present in sea water are killed in just single pass through the

cavitation element (orifice plate). By further optimizing the operation of cavitation element and by increasing the number of passes it is very easily possible to achieve complete (100%) disinfection of zooplankton. This, once again proves the utility of hydrodynamic cavitation for zooplankton disinfection in sea water disinfection.

Among the zooplankton, decapod numbers are reduced to zero after being subjected to cavitation in orifice plates. The decrease in numbers of copepod and cirripede nauplii is also substantial with the decrease in the open valve area. Also, Favella numbers are reduced to zero with 75% open area of orifice plate. However, bivalve and gastropod larvae were not affected in any of the conditions (Fig. 6) currently used.

(Fig. 6 here)

The experimental value of disinfection obtained in three conditions of orifice is almost similar in spite of wide differences in their cavitation numbers (Table 1). A constant extent of killing in all the orifice configurations can be explained based on cell wall strength of zooplankton and transient nature of cavitation. Most of the zooplankton develop hard skeletons, which are either external or internal. The exoskeletons are either chitinous as in the crustacea or calcareous as in the larval mollusks or brachiopods [19]. The zooplankton mainly in the influent seawater consisted of worms, mollusks and arthropods; the major component of the cuticles and exoskeletons is made up of chitin, which is one of the most abundant polysaccharides in nature [20]. The gradient in the stiffness and hardness through the cuticle thickness are interpreted in terms of honeycomb mechanism of the twisted plywood structure which is formed by the helicoidal stacking sequence of the fibrous chitin-protein layers [21].

Empirical equation for extent of killing

Here we develop a correlation which relates the extent of killing of zooplankton with geometrical parameters, operating parameters, cavity dynamics & cell characteristics.

Cell wall strength is an important parameter which controls the extent of disruption of cell. Although no information about cell wall strength of zooplankton is available in literature we try to correlate the stress generated by a cavity to obtain the wall strength on the basis of the disinfection results obtained from the present experiments. In the empirical equation we include a term

$$\exp\left(-S_{cell}\Big/\Delta P_{cavity}\right) \tag{16}$$

This term takes into account the cell wall strength (S_{cell}) and stress generated by a cavity (ΔP_{cavity}) which is obtained from cavity dynamics simulations. This term gives probability of killing (disruption) of cell with strength 'S_{cell}' Pa when subjected to a stress of 'ΔP_{cavity}' Pa.

As discussed earlier, Cavitation number is an important operating parameter which controls intensity of cavitation. Cavitation devices are usually operated at a value of cavitation number lower than the inception cavitation number and larger than choked cavitation number. Inception cavitation number is dependent on dissolved gases and suspended solids present in liquid. It is also a function of geometry of cavitational device [22]. However for a particular case of wastewater or ballast water treatment (sea water), which has a lot of ready nuclei in the form of dissolved gases and suspended solids, cavitation can be initiated even at very high values of cavitation number. This fact is also confirmed from the experimental results of case 'III' where cavitation number is 14.6, yet almost 82% of the zooplankton are killed. The lower limit for operating cavitation

number is the choked cavitation number. At choked cavitation number very large numbers of cavities are generated. Such a large number of cavities tend to damp the energy released by the neighboring cavity collapse. Thus the net energy available for cell disruption decreases. Hence cavitation device should be operated at a cavitation number higher than choked cavitation number. Balasundram & Harison (2006) [6] have observed decrease in the extent of yeast cell disruption at a very low value of cavitation number. In the present case following term is included which takes into account the operating parameter of cavitation device in form of cavitation number and choked cavitation number.

$$\exp\left(-C_{CN}\Big/C_{VN}\right) \qquad (17)$$

Choked cavitation number is calculated from following equations [22]

$$C_{CN} = 2\left(\frac{A_O}{A_P}\right)^2\left(\frac{A_P}{A_O}\frac{1}{Cc}-1\right) \qquad (18)$$

Where, C_C is contraction coefficient and is given as

$$C_c = 0.62 + 0.38\left(\frac{A_O}{A_P}\right)^3 \qquad (19)$$

Dynamic behavior of a cavity is controlled by the fluid turbulence in the downstream of an orifice. Size of dominant turbulent eddies is related to the size of orifice as '0.07 d_o', where, d_o is the size of orifice. While the turbulent eddies are seen to be generated from the periphery of the liquid jets being issued from the orifice plate. Thus, the perimeter of the holes in the orifice plate determines the shear layer that is generated in the downstream of the orifice. We include the effect of geometrical parameters in the equation in the form of following term

$$\left(\frac{P_h \times 0.07 d_o}{A_P}\right) \tag{20}$$

The terms given in formulae (16), (17) & (20) can be combined in form of following equation to predict the extent of cell disruption (X) when sea water is once passed through the cavitation device.

$$X = K.\exp\left(\frac{-S_{cell}}{\Delta P_{cavity}}\right).\exp\left(\frac{-C_{CN}}{C_{VN}}\right)^A \cdot \left(\frac{P_h \times 0.07 d_o}{A_P}\right)^B \tag{21}$$

ΔP_{cavity} is obtained from equation (15) on the basis of cavity dynamics simulations. The coefficients K, A & B and cell wall strength 'S_{cell}' is obtained from data fitting and final form of equation is obtained as

$$X = (5.5).\exp\left(\frac{-117}{\Delta P_{cavity}}\right).\exp\left(\frac{-C_{CN}}{C_{VN}}\right)^{1.11} \cdot \left(\frac{P_h \times 0.07 d_o}{A_P}\right)^{0.38} \tag{22}$$

Figure 7 shows comparison of experimental and predicted values of extent of disruption of zooplankton and a fairly good agreement with the experimental values is seen. Wall strength of zooplankton is obtained to be 117 Pa. Although this value seems to be very low but it should be brought to the notice of readers that only the localized stress of 117 Pa acting on comparative to the length scale of microbe can bring about killing and not the bulk stress. To generate turbulent stress of 117 Pa in ballast water flowing through the pipe the required turbulent fluctuating velocity is 0.48 m/s (Stress = $\frac{1}{2}\rho v'^2$). Thus if water is flowing at 2 m/s then the required turbulent intensity is 24% (0.48/2), which is unusually high for a pipe flow thus zooplankton are not likely to be killed in flow through pipe. Such a turbulent intensity can exist inside a pump hence in the present case almost 28% of the zooplankton were killed when water was pumped without cavitation device and valve kept fully open in case of control experiment.

Energy wise comparison of performance of cavitation device

Table 3 presents energy wise comparison of various configurations of the experimental setup. We consider 1 m^3 of sea water to be treated in order to reduce the zooplankton count to 5% of the initial count with the current designs of cavitation elements. Extent of killing of zooplankton for single pass (X) through various configurations is known, thus we can find out the number of passes ($N_{5\%}$) required to reduce the number of zooplankton to 5% of initial number density as

$$N_{5\%} = \frac{Ln\,(0.05)}{Ln\,(1-X)} \tag{23}$$

The number of required passes thus calculated is shown in table 3. It is seen that almost 10 number of passes are required when the sea water is passed through valve kept 100% open (case VI) as against just 2 passes when sea water is passed through the various orifice configurations (case I, II & III). Thus the Energy required for treating sea water in various valve configurations is almost 2-3 times higher than the energy required for orifice configurations. As described earlier the stress required to kill a zooplankton can also be generated in a pump or a valve. But it is seen in the present study that the required turbulent shear stress can be generated in a very energy efficient manner by volumetric oscillations of the cavities in the downstream orifice plates by creating hydrodynamic cavitating conditions.

7. Conclusion

Several mechanisms for cell disruption including impingement on solid surface, high velocity liquid jet, shock wave are proposed in the literature. In the present

investigation, the observations on the cavity dynamics revealed that a cavity undergoing rapid volumetric oscillations could produce high turbulence shear stress in the surrounding liquid. Thus, the cavitation occurring in the system can produce several effects, such as high velocity liquid jet, shock wave and turbulent shear stress, which are responsible for cell disruption. Following conclusions can be drawn from present study

1. Cavitation is shown to be an effective tool for seawater disinfection. More than 75% of the Zooplankton present in the seawater were killed by subjecting them to cavitation and/or turbulent fluid shear by flow though orifice. The cavitation devices being simple flow devices can easily be scaled up and hence can be used for large-scale cell disruption, microbial wastewater treatment and ballast water treatment.

2. Cavitation number is a simple and fast tool to quantify the extent of cavitation taking place in the various cavitational devices.

3. Cavitation occurring in the pipe fittings like valves was also quantified in terms of zooplankton mortality. Energy efficiency of zooplankton mortality using orifice plate was seen to be much higher than that in partially closed valve or in pump.

4. Theoretical model for quantifying the cavitational intensity & the extent of microbial cell disruption has been developed. The model correlates the turbulence energy dissipation rate due to rapid volumetric oscillations, operating cavitation number, geometrical parameters and cell strength with the extent of cell disruption.

Acknowledgements

Nomenclature

a, b	=	Constants in Vander Valls equation of state (Pa kgmol/m^3, m^3/kgmol)

a, b = Constants in Vander Valls equation of state (Pa kgmol/m^3, m^3/kgmol)
A_O = Open area in constriction, orifice area (m^2)
A_P = Area of pipe (m^2)
C = Velocity of sound in liquid phase (m/s)
C_C = Contraction coefficient
C_{CN} = choked cavitation number
C_{vn} = Cavitation number
D = Cell count in discharge water (post-cavitation) (m^{-3})
d_O = dimension of opening/ diameter of holes in orifice (m)
F = Constants in equation (6)
g = Acceleration due to gravity (m/s^2)
I = Cell count in intake water (pre-cavitation) (m^{-3})
k = Turbulent kinetic energy (m^2/s^2)
l_{eddy} = Turbulent eddy length scale (m)
n = Moles of gas in bubble (kgmol)
$N_{5\%}$ = Number of passes to reduce the microbial count to 5% of initial
P = Pressure (Pa)
ΔP = Shear stress developed by cavity (Pa)
P_h = Perimeter of open area/ perimeter of holes (m)
P_v = Partial pressure of vapor in bubble (Pa)
R = Radius of bubble (m)
Rg = Gas law constant (Pa.m^3/K/kgmol)
S = Bubble wall velocity (m/s)
S_{cell} = Cell wall strength (Pa)
T = Temperature (K)
t = Time (s)
V, v = Liquid velocity (m/s)
Vol = Volume (m^3)
We = Weber number
X = Extent of killing of zooplankton
Z = Potential head associated with incoming/outgoing mass (m)
ρ = Density (kg/m^3)
σ = Surface tension (N/m)
ε = Turbulence energy dissipation rate (m^2/s^3)
μ = Viscosity of liquid (kg/m/s)

Subscript
B = Bubble
cell = Microbial cell
∞ = Liquid at infinity
l = Liquid phase

Superscript
$'$ = Fluctuating

References

[1] R.H. Perry, C.H. Chilton, 1973. Chemical Engineer's Handbook, Fifth edition. Mc-Graw Hill Publications, 1973, pp. 5-36.

[2] V.S. Moholkar, A.B. Pandit, Bubble behavior in hydrodynamic cavitation: Effect of turbulence, AlChE Journal 43 (6) (1997) 1641-1648.

[3] S.S. Save, A.B. Pandit, J.B. Joshi, Microbial cell disruption: role of cavitation, The Chem. Engg. J. 55 (1994) B67-B72.

[4] A.C. Anil, K. Venkat, S.S. Sawant, M. Dileepkumar, V.K. Dhargalkar, N. Ramaiah, S.N. Harkantra, Z.A. Ansari, Marine bioinvasion: Concern for ecology and shipping, Curr. Sci. 83(3) (2002) 214-218.

[5] K.K. Jyoti, A.B. Pandit, Water disinfection by acoustic and hydrodynamic cavitation, Bio. Chem. J. 7 (2001) 201–212.

[6] B. Balasundaram, S.T.L. Harrison, Disruption of Brewers' Yeast by Hydrodynamic Cavitation: Process Variables and Their Influence on Selective Release, Biotechnology and Bioengineering, 94(2) (2006) 303-311.

[7] Y. Yan, R. B. Thorpe, Flow regime transitions due to cavitation in the flow through an orifice. Intl. J. of Multiphase Flow. 16 (1990) 1023-1045.

[8] C.R. Engler, C.W. Robinson, Effects of organism type and growth conditions on cell disruption by impingement, Biotechnology Letters 3 (2) (1981) 83-88.

[9] T. Keshavarz, R. Eglin, E. Walker, C. Bucke, G. Holt, A.T. Bull, M.D. Lilly, The large scale immobilization of Penicillium chrysogenum: Batch and continuous operation in an air lift reactor, Biotechnology and Bioengineering 36 (8) (1990) 763-770.

[10] M.S. Doulah, Mechanism of biological cells in Ultrasonic cavitation, Biotechnology and bioengineering XIX (1977) 649-660.

[11] A. N. C. R. Kolmogoroff, Acad. Sci. URSS 30 (1941) 301.

[12] C.F. Naude, A.T. Ellis, On the mechanism of cavitation damage by non-hemispherical cavities in contact with a solid boundary, ASME. J. Basic Eng. 83 (1961) 648-656.

[13] T.B. Benjamin, A.T. Ellis, The collapse of cavitation bubbles and the pressures thereby produced against solid boundaries, Phil. Trans. Roy. Soc., London, Ser. A 260 (1966) 221- 240.

[14] Rayleigh, On the pressure developed in a liquid during the collapse of a spherical cavity, Phil. Mag. 34 (1917) 94.

[15] M.S. Plesset, The dynamics of cavitation bubbles, ASME J. Appl. Mech. 16, (1948) 228-231.

[16] A. Shima, Y. Tomita, The behavior of a spherical bubble in mercury/report 2. The Reports of the Institute of High Speed Mechanics 39. Sendai, Japan: Tohoku University, (1979) 19-45.

[17] D.A. Lewis, J.F. Davidson, Bubble sizes produced by shear and turbulence in a bubble column, Chem. Engg. Sci. 38 (1983) 161-167.

[18] S.N. Gastgar, M Chem Engg Thesis, University of Mumbai, 2004

[19] A. Hardy, The open sea, Houghton Mifflin, Boston (1956) 335.

[20] C. Je uniaux, Bull. Soc. Zool. Fr. 107 (1982) 363-386.

[21] D. Raabe, C. Sachs, P. Romano, The crustacean exoskeleton as an example of a structurally and mechanically graded biological nanocomposite material, Acta. Materialia. 53 (2005) 4281-4292.

[22] C. Mishra and Y. Peles, Cavitation in flow through a micro-orifice inside a silicon microchannel, Physics of Fluids, 17 (2005) 013601-15.

Table captions

Table 1 - Experimental details of various orifice & valve configurations

Table 2 - Parameters used for theoretical predictions of extent of killing of zooplankton

Table 3 - Energy wise comparison of performance of various configurations
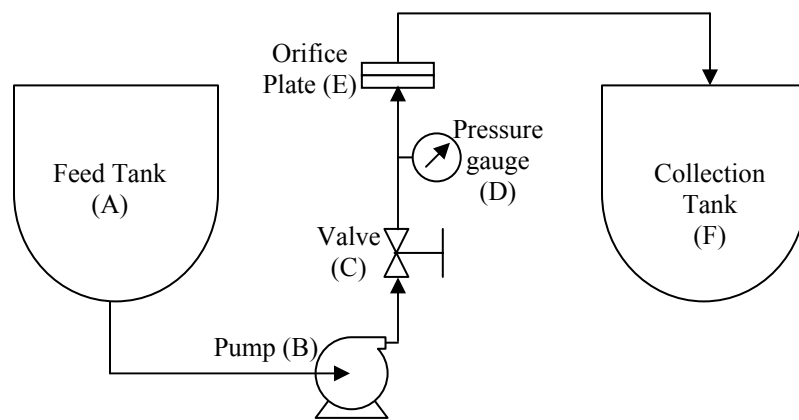
Figure captions

Fig. 1 - Schematic of the experimental set up (A - Feed tank; B- centrifugal pump; C-
Flow regulating valve; D- Pressure guage; E- Cavitation element (Orifice); F-
Collection tank)

Fig. 2 - Different configuration of orifice plates and valves. Shaded region shows open
area in the constriction

Fig. 3 - Typical pressure profile in orifice (Cavitating device) (Point 1 – upstream of the
orifice; Point 2 - vena contracta; Point 3 - downstream of the orifice)

Fig. 4 - (a) Division of cavity into thermal regions, (b) Temperature profile across
bubble-liquid interface into thermal regions

Fig. 5 - Cavity dynamics of 10μm cavity (a) orifice configurations (b) valve
configurations

Fig. 6 - The influence of cavitating conditions created by (a) differential pump valve
opening and (b) created by flowing through a cavitating element (orifice plates)
on the survival of zooplankton.

Figure 7: shows comparison of experimental and predicted values of extent of killing of
zooplankton

Fig. 1 - Schematic of the experimental set up (A - Feed tank; B- centrifugal pump; C-Flow regulating valve; D- Pressure guage; E- Cavitation element (Orifice); F- Collection tank)
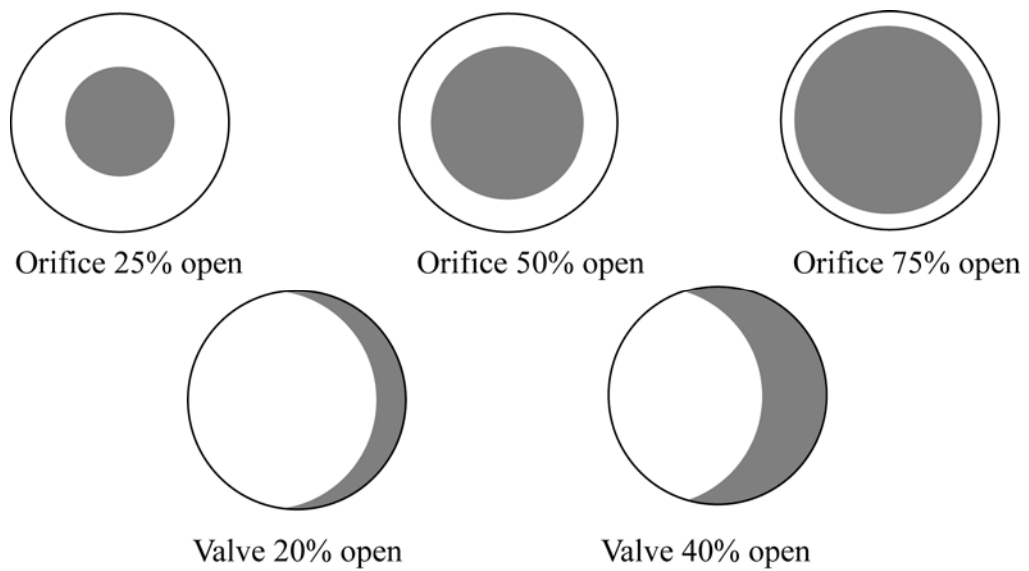
Fig. 2 - Different configuration of orifice plates and valves. Shaded region shows open area in the constriction
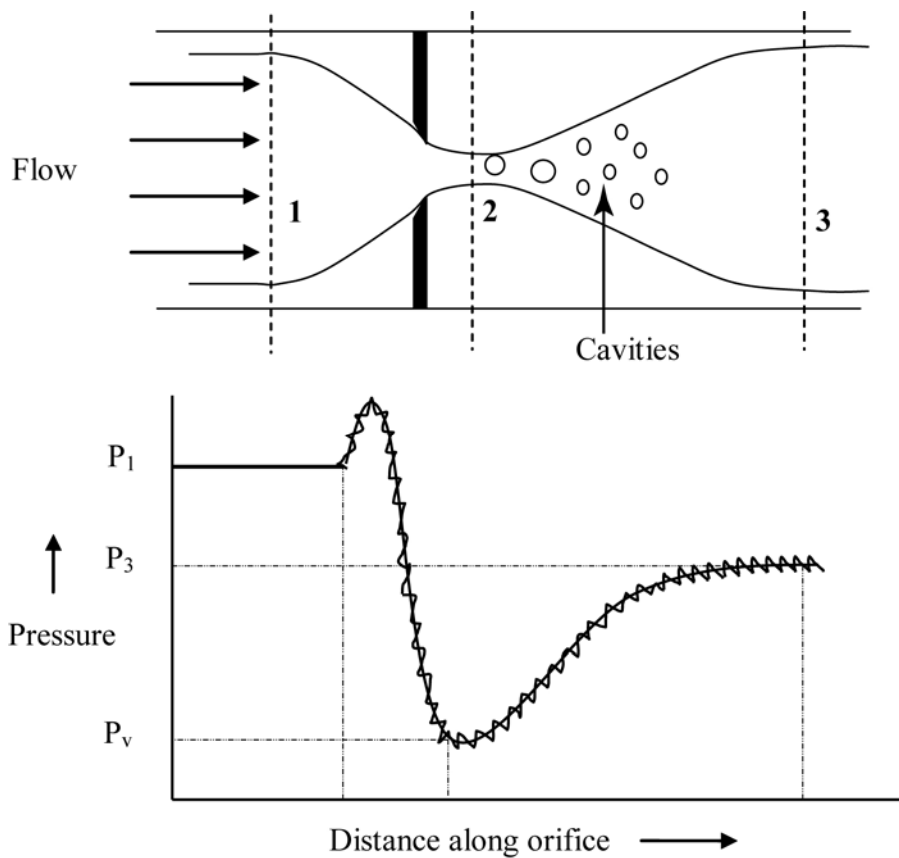
Fig. 3 - Typical pressure profile in orifice (Cavitating device)
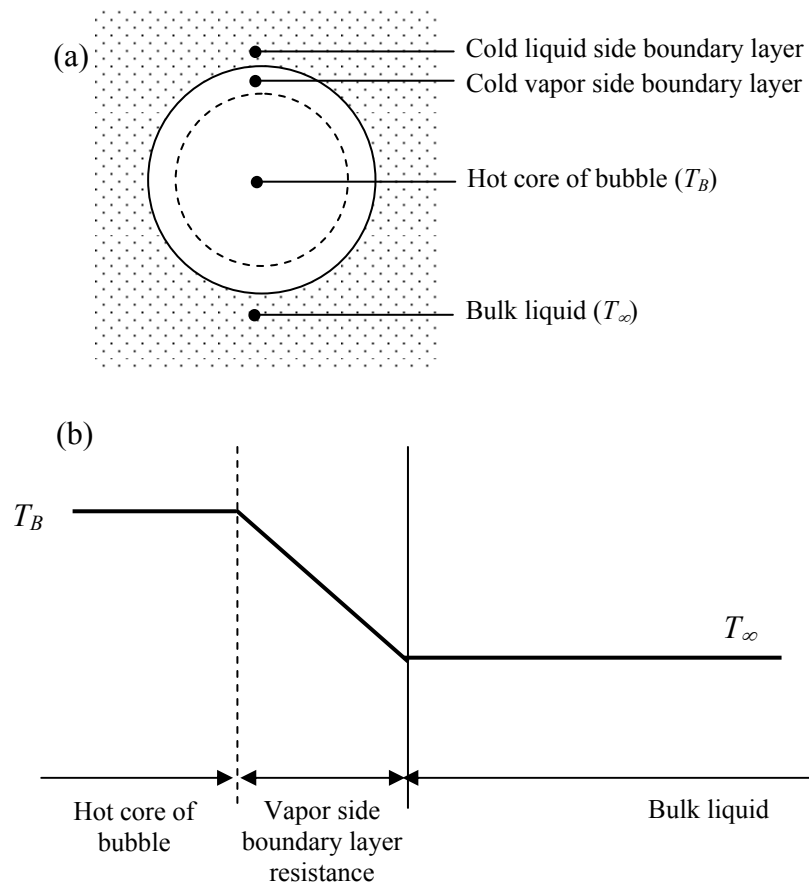(Point 1 – upstream of the orifice; Point 2 - vena contracta; Point 3 - downstream of the
orifice)

Fig. 4 - (a) Division of cavity into thermal regions, (b) Temperature profile across bubble-liquid interface into thermal regions
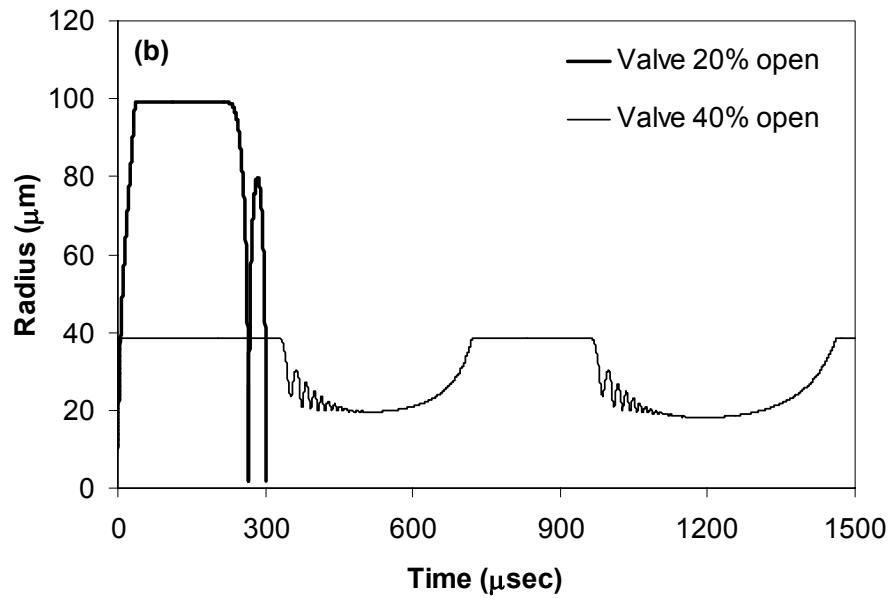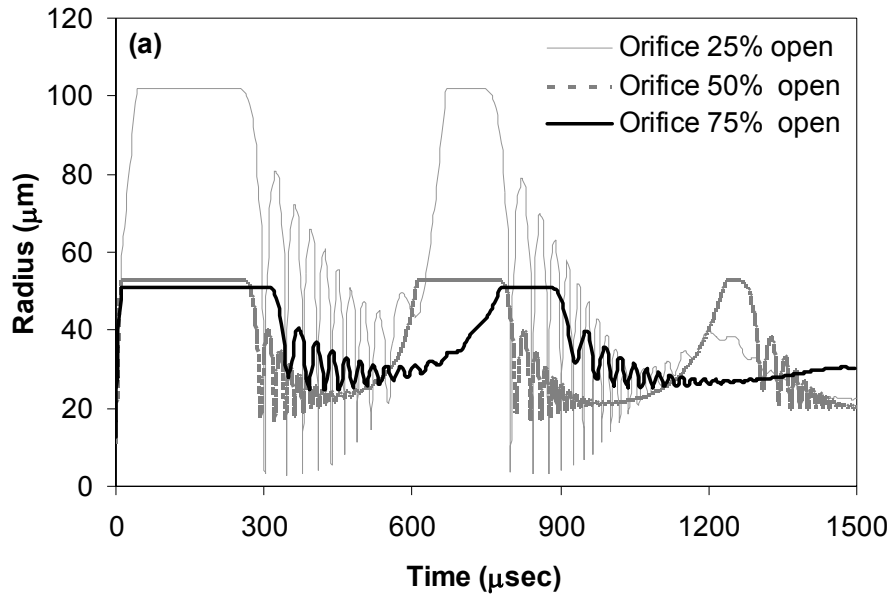
Fig. 5 - Cavity dynamics of 10μm cavity (a) orifice configurations (b) valve configurations
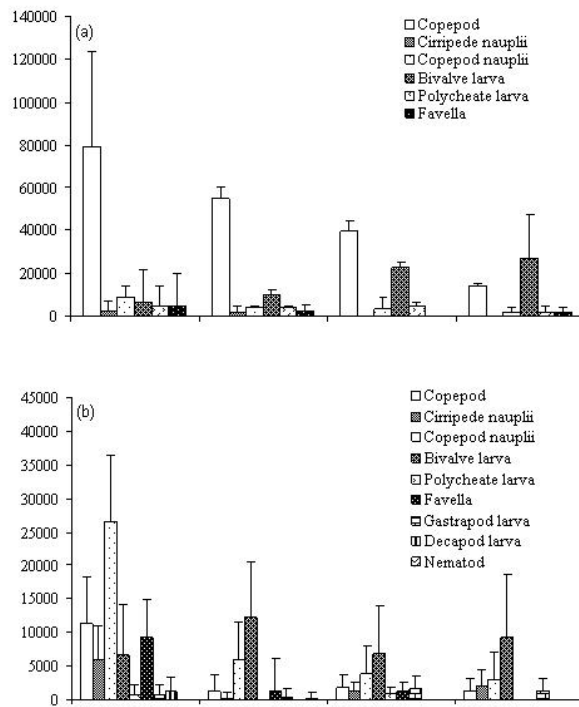
Fig. 6 - The influence of cavitating conditions created by (a) differential pump valve opening and (b) created by flowing through a cavitating element (orifice plates) on the survival of zooplankton.
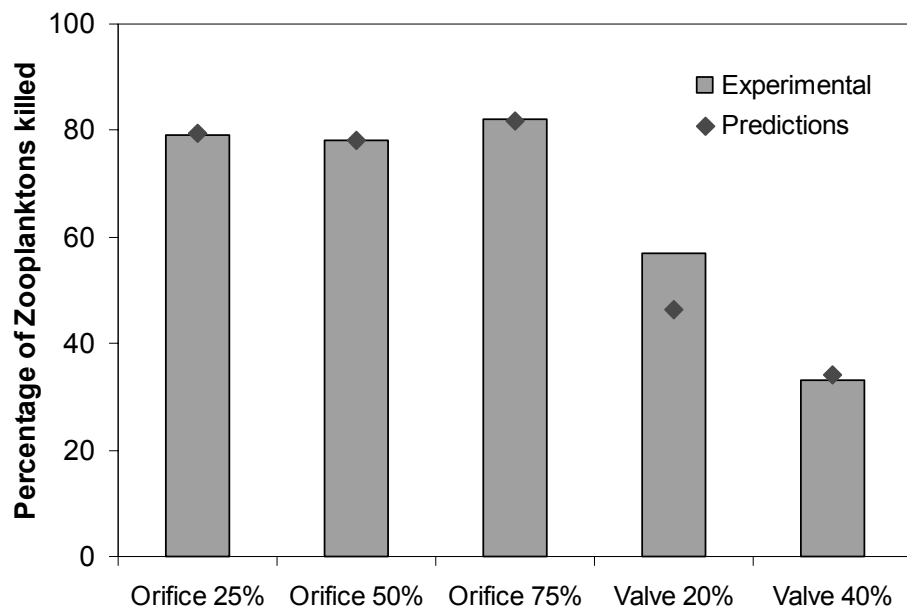
Figure 7: shows comparison of experimental and predicted values of extent of killing of zooplankton

Case	Geometry	Open area (%)	killing (%)	Pressure (kg/cm^2)	Flowrate (l/s)	Velocity at constriction (m/s)	Dimension of opening (mm)	Perimeter of open area/ perimeter of holes (mm)
I	Orifice	25	79	3.8	0.8	10.19	10.0	31.40
II	Orifice	50	78	3.3	1.7	10.83	14.1	44.41
III	Orifice	75	82	3.2	1.3	5.52	17.3	54.39
IV	Valve (4 turns closed)	20	57	3.5	1.0	15.95	2.7	28.24
V	Valve (3 turns closed)	40	33	3.3	1.9	15.13	5.9	24.90
VI	Valve (full open)	100	28	3	2.8	-	-	-

Table 1 - Experimental details of various orifice & valve configurations

Table 2 - Parameters used for theoretical predictions of extent of killing of zooplanktons

Case	Choked Cavitation number (C_{CN})	Cavitation Number (C_{VN})	Turbulent fluctuating velocity (m/s)	Average turbulence energy dissipation rate of cavities ($\bar{\varepsilon}$) (m^2/s^3)	Stress generated by cavity ΔP_{cavity} (Pa)	Predicted extent of killing (%)
I	0.67	5.13	1.27	22627	150.4	79.5
II	1.00	3.94	1.77	16018	126.5	78.0
III	0.80	14.68	1.71	8717	93.3	81.7
IV	0.56	1.93	1.29	36994	192.3	46.3
V	0.92	2.02	2.06	14510	120.4	34.2

Table 3 - Energy wise comparison of performance of various configurations

Case	Cavitation device	Flow rate (lit/s)	Time required for single pass of 1 m^3 of sea water (sec)	Extent of Disruption in Single pass (%)	No. of Passes to achieve 95% Killing	kW.hr for required no. of passes
I	Orifice	0.8	1250	79	2	3.85
II	Orifice	1.7	588	78	2	1.81
III	Orifice	1.3	769	82	2	2.37
IV	Valve	1	1000	57	4	6.17
V	Valve	1.9	526	33	8	6.49
VI	Valve	2.8	357	28	10	5.51